Faceting in directional solidification

Mokhtar Adda Bedia and Martine Ben Amar
Laboratoire de Physique Statistique de L'Ecole Normale Supérieure, 24 rue Lhomond, 75231, Paris CEDEX 05, France
(Received 26 November 1990)

We examine the growth of a faceted crystal in the cellular regime of directional solidification. We prove, both by a model and by a complete numerical solution, the existence of faceted cusplike cells and the possibility of maintaining a Saffman-Taylor picture at least for the tip. Faceting does not modify the usual selection mechanism and the wavelength of the pattern remains unpredicted.

We present here a treatment of faceted crystal growth far from equilibrium. We chose the case of directional solidification in the cellular regime for its great practical interest, for example in the case of semiconductors. Such a free-boundary problem with volume diffusion in the liquid phase and specific interface laws has apparently never been solved before, although as early as 1951, Herring,[1] analyzed the set of equations of a closely related problem and argued that a solution should exist. During the last decade, numerous theoretical[2] and numerical works[3] have been devoted to stationary diffusive instabilities giving rise to rough interfaces. All of them emphasize the crucial role of surface tension in selecting specific solutions among a continuum of possible crystal shapes. More precisely, what is involved is the surface tension stiffness given by $\gamma(\theta)+\gamma''(\theta)$, θ being the angle between the growth and the crystal normal directions. Most of the time, thermodynamical equilibrium of the interface is assumed. So, Dirichlet (like the Gibbs-Thomson law) and Neuman (like the Stéfan law) conditions have to be applied to the interface which is an unknown function fixed by the experimental growth conditions. In directional solidification, its shape is dominated by the volume diffusion of the impurities, which amount is characterized by $(c_1-c_\infty)/(c_1-c_s)$ (where c is the impurity concentration and the denominator is the miscibility gap Δc as given by the phase diagram). The interface is stabilized by the exterior temperature gradient G and by the capillary effects. Here, we will speak mostly in terms of impurity concentration, although all the physical considerations in the following can be applied to the thermal solidification of a pure sample, in the dendritic context for example.[4] Only morphological aspects are specific to the directional solidification case.

When the experiment takes place below the roughening temperature $T_R(\mathbf{n}_0)$ of some specific direction $\mathbf{n}_0$, the crystal displays a facet.[5] Contrary to the rough part of the crystal, the local impurity amount (or supersaturation) cannot be fixed for each point of the facet since its shape, a segment in two dimensions, is perfectly known. Only the mean value of this amount[1,4] is imposed and gives the facet length, but not in an obvious way. It depends both on the surface tension cusp ϵ_0 of the Wulff's plot[1] and on attachment kinetics. for faceted parts of the crystal, the kinetic is not instantaneous so a facet inhibits the growth and requires a specific local supersaturation which depends upon the detailed growth mechanism: dislocations[6] or bidimensional terrace nucleations.[7] Note that, from a purely mathematical point of view, only the existence of a cuspoidal point in the Wulff's plot is responsible for faceting in a crystal. In the following, as usual, we will assume that the physical parameters, such as ϵ_0, are only weakly dependent on the temperature. This is a reasonable assumption if the experiment is made well below the roughening temperature. In this case the growth of the facets is mostly dominated by dislocations and we avoid the difficult situation of the roughening transition as considered in Ref. 7.

We decided to treat an example of steady-state faceted crystal growth in the fully nonlinear regime. The linear stability of the faceted crenellated front, for two orientations θ_0 of the facet, have been examined in Refs. 8(a) and 8(b). They found solutions of small extension beyond the usual Mullins-Sekerka[2] threshold: $\nu_{\mathrm{MS}}=m\Delta cU_{\mathrm{MS}}/G2D\approx 0.5$, with D the diffusion coefficient in the liquid phase, m the absolute value of the slope of the solidus given by the phase diagram, and U the pulling speed. As suggested by experiments on weakly anisotropic materials,[9] we considered a cusplike cell pattern with two facets at $\theta_0=\pm 45°$ of the velocity U. We computed infinite steady-state cells by solving the integrodifferential equation which comes from the Green's-function formulation of directional solidification.[2] The treatment of the rough parts of the cell have been explained in great details in Ref. 10. On the facet, we used the averaged Gibbs-Thomson law as emphasized in Ref. 4. Our main results are the existence of such cells (see an example in Fig. 1) for a surface tension less than a maximum value at fixed cusp value ϵ_0. To interpret our numerical results, we have adapted an analytical treatment of directional solidification given in Ref. 11. It relies on a viscous fingering analogy, valid at low Péclet numbers $P=\alpha U/D$, α being the wavelength of the pattern. Even with facets, we found again known results concerning the Saffman-Taylor (ST) finger and the directional solidification cellular regime. In particular, we prove the existence of a maximum surface tension for the two faceted instabilities while the pattern wavelength remains unpredicted by this steady-state treatment. Faceting does not introduce a new kind of selection

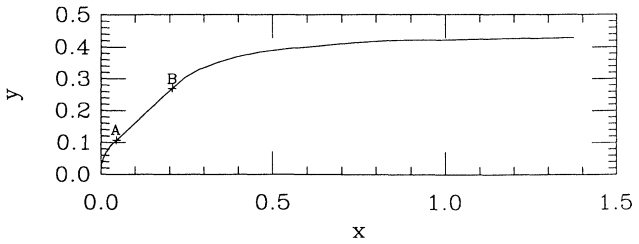

FIG. 1. Numerical faceted cell, solution of the half-profile equation for $\sigma=0.0033$, $P=0.2$, $\epsilon=0.5$, and $\nu=1$. Definition of our coordinate frame and of our profile partition A and B.

mechanism: it does not restrict the space of solutions, rather it increases it since it introduces its own physical parameters such as ϵ_0. This model which explains our numerical results also explains the decrease of the facet length when the growth rate increases, an experimentally observed result.

The boundary-layer analysis,[11] valid in the vanishing $(1-\lambda)$ limit, splits the cell profile in two parts: the tip for $\theta \leq \pi/2$ and the grooves for $\theta \approx \pi/2$. The cell tip has an extension of order one (the wavelength of the pattern α is our length unit). When $\lambda \rightarrow 1$, it is well described by one of the pendulum solutions defined in (2) below, since the rescaled diffusion field is approximately linear in x (see Fig. 1). It reaches its asymptotic behavior in the second part, on distances of order $(1-\lambda)^{-1/3}$ which is assumed to be small when compared to the characteristic length scale $1/P$ of the grooves. The asymptotic matching procedure[11] proves that the surface tension fixes the parameter λ of the equivalent ST finger while the Péclet number is left arbitrary. Since the facets occur in part one ($\theta_0 \ll \pi/2$), our treatment of faceting modifies only the tip region and not the grooves, therefore, our analysis focuses mainly on the cell tip.

It is time now to specify our surface tension. For this, we will assume the simplest singular function: $\gamma=\gamma_0(1+\epsilon_0 \sin|\theta \pm \theta_0|)$. In this case, the surface tension stiffness $\gamma+\gamma''$ is constant for all crystal directions except for $\theta=\pm\theta_0$. The matching of the rough parts with the facet are smooth since the stiffness is positive everywhere. The profile exhibits only a singularity of the curvature, in the vicinity of θ_0. Due to the linear behavior of the impurity concentration field, valid to leading order in P, rough parts of the tip are deduced from the Gibbs-Thomson law,

$$\omega_0-\sigma[\mathcal{K}_{\rm int}+\beta F(P\cos\theta)]=x_{\rm int}$$

$$\text{with } \sigma=\frac{T_m(\gamma+\gamma'')}{G\alpha^2(2\nu-1)} \quad (1)$$

with $\mathcal{K}_{\rm int}$ the positive curvature of the interface and T_m the melting temperature of the pure sample. σ is the dimensionless surface tension parameter that must be identified to the ST parameter.[10,11] In (1), $(2\nu-1)$ means the deviation from the Mullins-Sekerka threshold. β, the kinetic coefficient is scaled by the surface tension parameter so each term in (1) has no dimension. For atomically rough interfaces, $F=P\cos\theta$, and attachment kinetics must not be taken into account in (1). Hereafter, we will call part A the rough cell tip, part B the facet, and part C the end of the cell tip before the beginning of the groove (Fig. 1). From (1), we deduce the half profile of part A and C, the whole profile is obtained by symmetry about the x axis. In part A,

$$x(\theta)=(2\sigma)^{1/2}[(1+C_A)^{1/2}-(\cos\theta+C_A)^{1/2}] ,$$

$$y(\theta)=\sigma^{1/2}\Psi(\theta,C_A)$$

with

$$\Psi(\theta,C_A)=2^{-1/2}\int_0^\theta d\theta' \frac{\cos\theta'}{(\cos\theta'+C_A)^{1/2}} . \quad (2)$$

θ is less than θ_0 which defines the beginning of part B. For the moment, C_A is an unknown constant of integration. The profile in part B is known: it is a line segment which begins at the point $A(X_A,Y_A)$ and stops at $B(X_B,Y_B)$ such that $Y_A-Y_B=\cot(\theta_0)(X_A-X_B)$. X_A and Y_A satisfy (2) for $\theta=\theta_0$, the facet orientation. Finally, in part C of the cell

$$x(\theta)=(2\sigma)^{1/2}[(\cos\theta_0+C_C)^{1/2}-(\cos\theta+C_C)^{1/2}]+X_B ,$$

$$y(\theta)=\sigma^{1/2}[\Psi(\theta,C_C)-\Psi(\theta_0,C_C)]+Y_B .$$

When applied both on the left- and right-hand sides of the facet, relation (1) gives the facet length l_0,

$$l_0=\sigma^{1/2}\mathcal{L}$$

$$=\frac{2\sigma^{1/2}[(\cos\theta_0+C_A)^{1/2}-(\cos\theta_0+C_C)^{1/2}]}{\sin\theta_0} .$$

Clearly, $C_A \geq C_C$. At the end of part C, the tip almost completely fills the cell, $\theta \approx \pi/2$, and the profile has to be matched to the asymptotic part. The matching is made possible if C_C is negative and small.[11] The condition $y_C(\arccos|C_C|)\approx\frac{1}{2}$ gives the surface-tension coefficient in terms of the integration constants C_A and C_C,

$$\sigma^{-1}=4[\Psi(\theta_0,C_A)+\Psi(\arccos(|C_C|),C_C)-\Psi(\theta_0,C_C)$$

$$+\mathcal{L}\cos(\theta_0)]^2 . \quad (3)$$

The matching with the grooves leads to the selection of λ in terms of σ: $|C_C|\approx 2.17(1-\lambda)^{2/3}/\sigma^{1/3}$. In order to discuss this result, let us determine the facet length as a function of ϵ_0, the anisotropy coefficient. By performing the average of the Gibbs-Thomson relation (1) along the facet as suggested in Ref. 4, one derives the anisotropy coefficient in terms of the constants of the pendulum solution

$$(C_A-C_C)/\sin\theta_0=2\epsilon_0+\sigma^{1/2}\mathcal{L}\beta F(P\cos\theta_0)=\epsilon . \quad (4)$$

In (4), it is necessary to detail the kinetic supersaturation, negligible for the rough parts of the crystal. For a growth by dislocations, F behaves approximately like $P^{1/2}$ at low velocity (called hereafter the first regime of growth) and like P at increasing velocity (second regime).[6] Note that we must include it only in the first regime of growth and only on the facet, since our model

does not include linear corrections in P. The average of the kinetic supersaturation as in Ref. 4 can be questionable since it depends on the detailed microscopic mechanism of growth of the steps on the facet. Nevertheless, we do not know about any microscopic theoretical treatment which includes both capillary effects and an inhomogeneous diffusion field along the facet. Capillary effects are excluded in Ref. 6 and only Kokoyama and Kuroda[6] consider a varying "undercooling" in each point of the facet. Only capillary effects can explain the existence of a close-packed surface. We hope that Eq. (4) is valid, at least from a purely scaling point of view, and useful for a physical discussion. Let us now discuss these two regions of growth, starting with the second one.

(i) *Negligible kinetic effects:* $F \approx P$.

After linearization of Eq. (3) in the limit of vanishing $|C_C|$, we find without difficulty the ST parameter λ in terms of the surface tension,

$$\sigma = \sigma_{\max}(\epsilon_0)[1-\tau(\epsilon_0)(1-\lambda)^{2/3}] .$$

$\sigma_{\max}(\epsilon_0)$ is derived from Eqs. (3) and (4) with $C_A = 2\epsilon_0 \sin\theta_0$ and $C_C = 0$, and is the largest allowed surface tension for cusplike cells. λ identifies the ST finger which perfectly fits the cell tip, at least at low Péclet numbers. The expressions of $\sigma_{\max}(\epsilon_0)$ and $\tau(\epsilon_0)$ involve incomplete elliptic integrals and can be computed numerically. It is easy to check that $\tau(\epsilon_0)$ is always positive. In Fig. 2, we have plotted the theoretical facet length and the maximum surface tension for different ϵ_0. Also, in these figures numerical points, calculated with our code of directional solidification for various P values, are indicated. Note the nice agreement between the model predictions and the numerics and the weak effect of P. The most important result of our work is that with or without a cusp in surface tension, there exists an upper bound for the surface tension. Its value depends on the cusp amplitude. Its origin comes from the ST picture of directional solidification, valid at low Péclet numbers. Note that when $\lambda \neq 1$, at fixed ϵ_0, the facet length is reduced from its value at $\lambda = 1$. As expected, the maximum length is reached when both ϵ_0 and σ take their largest allowed value. This model does not allow facets greater than 0.405 for $\theta_0 = \pi/4$, even for $\epsilon_0 = 1$, although the geometry of the experiment allows a length of $2^{-1/2}$. Even for this particular value, the facet does not occupy the whole available space. To explain larger facets in directional solidification, one may put forward kinetic effects.

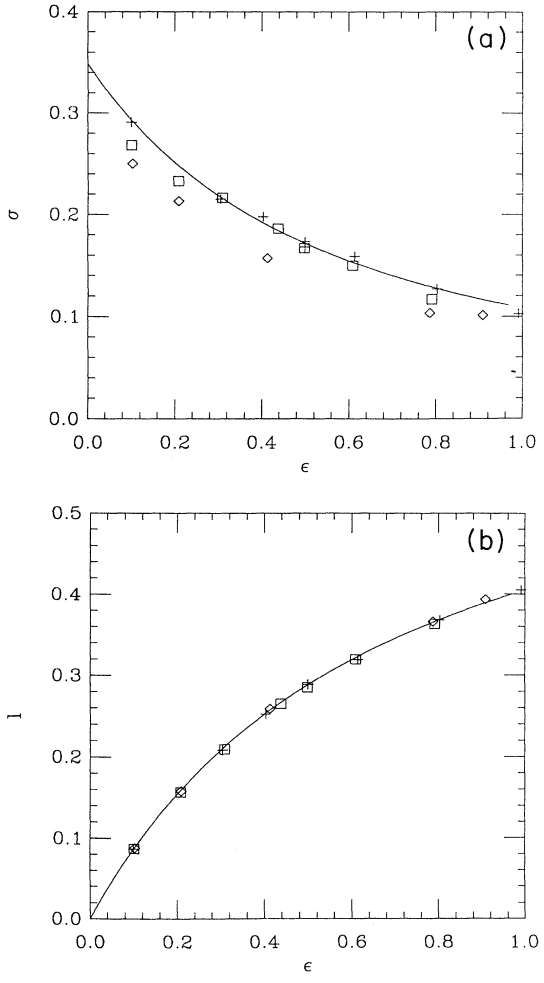

FIG. 2. Maximum value of the surface tension parameter σ (a) and the corresponding facet length l_0 (b) vs the anisotropy coefficient ϵ. ——, theoretical predictions for twice the value of the Mullins-Sekerka threshold and a coefficient of segregation equal to one. Numerical points: + for $P=0.01$, □ for $P=0.1$, ◇ for $P=0.4$.

(ii) *Kinetic effects included or the slow growth regime.* Once added in Eq. (4), the kinetic supersaturation increases the effect of ϵ_0 and the facet length. The effective ϵ, derived numerically and plotted in Fig. 2 is the result of both terms on the right-hand side of Eq. (4). Note that the facet length occupies the entire available space only if $\beta \to \infty$, that is when the capillary length vanishes. This limit is checked at very low growth rates and for highly anisotropic materials. For these, rough parts completely disappear of the periodic pattern. The observation of rough parts in the growing crystal like in Ref. 9 proves the necessity to include both volume diffusion and surface tension.

This purely kinematic model where the surface tension is independent of the temperature, contrary to any traditional dynamical roughening transition model, proves that the relative facet length decreases when the growth rate increases for two reasons: first, the dimensionless surface tension σ [Eq. (1)] decreases when one moves away from the Mullins-Sekerka threshold; second, at low velocity (first regime of growth), the kinetic "undercooling" is more efficient, as shown above. This can explain the visual disappearing of experimental facets at temperature rather below the roughening transition temperature. We hope that this work will suggest new experiments in directional solidification of weakly anisotropic materials.[9]

We gratefully thank V. Hakim, B. Moussallam, and Y. Pomeau for illuminating discussions, critical remarks concerning the manuscript, and continuous interest. The support by the Centre National d'Etudes Spatiales is greatly acknowledged.

[1]C. Herring, *The Physics of Powder Metallurgy,* edited by W. E. Kingston (McGraw-Hill, New York, 1951).

[2]J. Langer, Rev. Mod. Phys. **52**, 1 (1980) and *Chance and Matter,* edited by J. Souletie, J. Vanimenus, and R. Stora (North-Holland, Amsterdam, 1987); D. Kessler, J. Koplik, and H. Levine, Adv. Phys. **37**, 255 (1988); P. Pelcé, *Dynamics of Curved Fronts,* edited by H. Araki, A. Libchaber, and G. Parisi (Academic, London, 1988); Y. Pomeau and M. Ben Amar, *Solids Far from Equilibrium,* Beg-Rohu Lectures, edited by C. Godreche (Cambridge University Press, Cambridge, in press).

[3]D. Kessler, J. Koplik, and H. Levine, Phys. Rev. A **33**, 3352 (1986); D. Meiron, Phys. Rev. A **33**, 2704 (1986); M. Ben Amar and B. Moussallam, Physica D **25**, 155 (1987).

[4]M. Ben Amar and Y. Pomeau, Europhys. Lett. **6**, 609 (1988).

[5]W. K. Burton, N. Cabrera, and F. C. Frank, Philos. Trans. R. Soc. London Ser. A **243**, 299 (1951); P. Nozières, in *Solids Far from Equilibrium,* Beg-Rohu Lectures, edited by C. Godreche (Cambridge University Press, Cambridge, in press).

[6]A. A. Chernov, Usp. Fiz. Nauk **73**, 277 (1961) [Sov. Phys.—Usp. **4**, 116 (1961)]; E. Yokoyama and T. Kuroda, Phys. Rev. A **41**, 2038 (1990).

[7]P. Nozières and F. Gallet, J. Phys. (Paris) **48**, 353 (1987); D. Kessler and H. Levine (unpublished).

[8](a) R. Bowley, B. Caroli, C. Caroli, F. Graner, P. Nozières, and B. Roulet, J. Phys. (Paris) **50**, 1377 (1989); (b) P. Pelcé (unpublished).

[9]J. Maurer, P. Bouissou, B. Perrin, and P. Tabeling, Europhys. Lett. **8**, 67 (1988); E. Raz, S. G. Lipson, and E. Polturak, Phys. Rev. A **40**, 1088 (1989).

[10]M. Ben Amar and B. Moussallam, Phys. Rev. Lett. **60**, 317 (1988); M. Mashaal, M. Ben Amar, and V. Hakim, Phys. Rev. A **41**, 4421 (1990).

[11]T. Dombre and V. Hakin, Phys. Rev. A **36**, 2811 (1987).